PHYSICAL REVIEW B VOLUME 26, NUMBER 12 15 DECEMBER 1982

Model studies of oxygen-intercalated graphite

Aldona M. Butkus* and Cary Y. Yang†
Surface Analytic Research, Inc., 465 A Fairchild Drive, Suite 128, Mountain View, California 94043

Y. W. Tsang‡ and C. Y. Fong
Department of Physics, University of California, Davis, California 95616
(Received 30 November 1981; revised manuscript received 7 September 1982)

The possibility of intercalating oxygen to reduce the conductivity of graphite has been investigated by modified intermediate neglect of differential overlap 3 and tight-binding methods. The cluster calculations suggest that the most stable position for the oxygen atom is 1.25 Å above a carbon—carbon bond. The tight-binding band calculation predicts the stage-1 intercalated graphite to be a zero-indirect-gap semiconductor. Higher-stage intercalated graphite is expected to have a finite insulating gap whose value is governed by the carbon-oxygen interaction.

I. INTRODUCTION

Among the layered compounds, graphite has several unique properties for practical applications. First, its strong sp^2 bond between the carbon atoms in the basal planes renders graphite as a well-known lubricant. Second, the weak van der Waals interaction between the interlayer carbon atoms allows the material to be intercalated by various elements or molecules. The experimental evidences to date[1] indicate that the intercalated compounds are conductors and some of the compounds exhibit conductivities comparable to the best metallic conductors. Hence, many have explored the possibility of these compounds as substitutes for pure metal conductors. Finally, the fibrous form of graphite exhibits light weight and the ability to withstand stress. It has long been used as a lightweight high-strength material for aerospace applications and is being considered by the auto industry.

In the last application, the high conductivity of the graphite fibers could pose fire hazards during the disposal of the material. Therefore, in this work we specifically address the problem of reducing conductivity in graphite.

The high conductivity in the directions perpendicular to the principal ($\hat{z}$ or $\hat{c}$) axis in graphite originates from the overlap of the nonbonding $p_{\hat{z}}$ orbitals of the atoms held together by the saturated sp^2 bonds in the basal planes. This picture suggests that the conductivity may be reduced if the $p_{\hat{z}}$ orbitals were significantly distorted by intercalation. In terms of the $\vec{k}$-space picture, we introduce proper interaction between the p orbitals of the intercalant and the $p_{\hat{z}}$ orbitals of carbon such that the resultant band structure will be that of a zero-gap or a small-gap semiconductor. Keeping in mind that the intercalant should not significantly increase the weight of the material, we report in this paper the calculations of modeling oxygen intercalation in graphite. It is well known that the oxygen interacts extremely strongly with carbon. As Rüdorff[2] pointed out that it is possible to intercalate oxygen in graphite with a C:O atom ratio between 2.4 to 2.9. The oxygen atoms appear to favor the positions at the center of the hexagon.[3] In this paper, we adopted a complementary approach of using the modified intermediate neglect of differential overlap (MINDO) molecular-orbital method[4] and the Slater-Koster[5] (SK) tight-binding scheme. The former provides information about the stability of oxygen sites in the graphite, and the latter examines the effect of the different sites on the Fermi surface of the host graphite crystal by assuming an idealized C:O atom ratio. This ratio is equal to 2. A consistent model concerning the proper sites for the oxygen to reduce the conductivity is obtained by this approach. The tight-binding method has been used by Holzwarth[6] to study the validity of the rigid-band model of intercalated graphite. However, in the present studies, we are able to determine the most important interaction between the intercalant and the host crystal through which the conducting property of the material is altered.

In Sec. II, the methods of the calculations will be briefly presented. Results and conclusions will be given in Sec. III.

II. METHODS OF CALCULATIONS

A. Cluster model

In order to study the electronic structure of oxygen-intercalated graphite using a cluster-model approach, modified intermediate neglect of differential overlap (MINDO/3) (Ref. 7) molecular-orbital calculations have been carried out on clusters of carbon, hydrogen, and oxygen atoms modeling the oxygen-graphite system. The hydrogen atoms are used for handling the boundary problem of the cluster. The MINDO/3 approach was chosen because it allows one to obtain the ground-state solution to the Schrödinger equation for polyatomic systems in considerably less computation time. This savings over the *ab initio* Hartree-Fock-Roothaan molecular-orbital approach is achieved through either the neglect or the replacement by parameters of certain Hartree-Fock Hamiltonian matrix elements. These parameters have been previously determined through a lengthy iterative procedure by fitting experimental geometries and heats of formation for a large class of molecules.[4] In addition, since it is of interest in the present study to determine the optimum position for the oxygen atom in the graphite lattice, total-energy minimization as a function of atomic coordinates would be desirable and could be economically performed with the MINDO/3 approximation.

In choosing the cluster models of the oxygen-intercalant sites, preliminary calculations were carried out using the independent-layer model of the graphite lattice in order to determine possible oxygen binding sites. Models for the graphite layer ranged from a single ring of six carbon atoms to a condensed four-ring system. Hydrogen atoms at a carbon-hydrogen distance of 1.1 Å were used to saturate the dangling σ carbon bonds at the edges of the cluster models. Such a treatment of edge carbons was not expected to introduce serious errors since the oxygen-lattice interaction should mainly take place within the π-electron system. Additionally, energy differences between the lattice model and the lattice oxygen-intercalant model were of interest so that cancellation of errors due to the edge treatment was expected to occur. Use of the independent-layer model of the lattice further allowed the determination of the minimum cluster size necessary to adequately represent a property of interest.

Four different positions for the oxygen atom in the graphite lattice were considered and the cluster models chosen for study are indicated in Figs. 1—4.

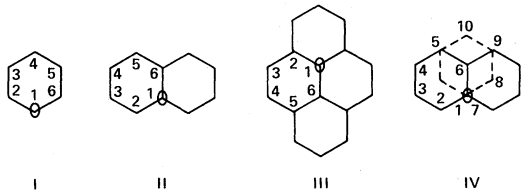

FIG. 1. Clusters chosen to model oxygen directly above carbon atom, site *A*. For the three-dimensional lattice model IV the upper graphite layer (C_7,C_8,C_9,C_{10}) is indicated by dashed lines. The oxygen atom is above C_1 in all structures. Hydrogens along the edges have been omitted for clarity.

The first, site *A*, places the oxygen directly above and below carbon atoms (Fig. 1). The second, site *B*, has the oxygen directly above a carbon and below the center of a hexagonal ring of the second layer (Fig. 2). Thus in the independent-layer models of this site, clusters are considered with the oxygen above a carbon as well as above the center of a ring of carbons separately. The oxygen can also be positioned above a carbon—carbon bond, site *C* (Fig. 3), which results in a position below a point midway between second-nearest neighbors of the second ring in the three-dimensional lattice model. The last oxygen-graphite site, *D* (Fig. 4), considered consists of the oxygen above and below the point midway between second-nearest neighbors of the hexagonal rings.

Before the oxygen-graphite calculations were done, the degree to which the various models of the lattice describe a perfect infinite system was checked. Two quantities often used are the valence charge residing on each atom, with a value of 4.00 for the ideal case, and the cohesive energy of the lattice, the negative of the binding energy with an experimental value of approximately 5 eV/atom.[8] This latter quantity is of particular interest since the previous theoretical studies of oxygen chemisorption[9] on graphite resulted in an overestimation of the lattice energy leading to the prescription of

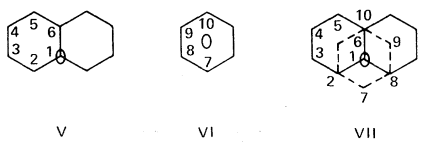

FIG. 2. Clusters modeling oxygen-graphite site *B*. The oxygen atom is above C_1 in structures V and VII. The upper graphite layer (C_7,C_8,C_9,C_{10}) in structure VII is indicated by dashed lines.

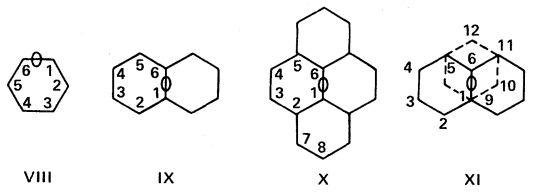

FIG. 3. Clusters modeling the bond-site position site *C*. Upper graphite layer (C_9,C_{10},C_{11},C_{12}) in structure XI is indicated by dashed lines.

arbitrarily dividing the binding energies by a factor of 5.

For all of the oxygen-graphite sites considered, MINDO calculations were first carried out on the simplest model of the lattice, a single ring of six carbon and six hydrogen atoms, obtaining the equilibrium oxygen to lattice distance. These values were then used for the calculations on the two ring models directly as well as reoptimized. Since the distances, charge distributions, and binding energies did not change significantly between the optimized and nonoptimized calculations, the oxygen-to-lattice distance was not redetermined in the larger structures of the two-dimensional lattice models. For the three-dimensional lattice models, the oxygen-lattice distance was again allowed to vary. All calculations were done within a rigid-lattice approximation. Binding energies for the oxygen atom were determined from the difference between the calculated heats of formation of the oxygen-graphite models, the analogous pure-graphite models, and the experimental value of 59.559 kcal/mole for the oxygen heat of atomization used in the parametrization procedure of MINDO. Electronic charges on the atoms were calculated using the Mulliken population approach.[10]

B. Band model

The SK tight-binding scheme was used to calculate the band structure of the oxygen-intercalated graphite. Since three of the four valence electrons on each carbon atom form a sp^2 covalent bond with its nearest neighbor within the x-y graphite layer, only the p_z orbital was included for the carbon atom in the basis states of the tight-binding Hamiltonian. For the oxygen atom, p_x, p_y, and p_z orbitals were used as the basis functions. For the case of pure graphite, the SK tight-binding Hamiltonian in terms of overlap integrals has matrix elements identical in form to the Slonczewski-Weiss-McClure[11,12] Hamiltonian, therefore, the overlap integrals in our scheme may be directly related to band-structure parameters that have been fitted to experimental Fermi-surface measurements given in the literature.[13] The correspondence between band parameters in the literature and the tight-binding overlap integrals are given in Table I; indices 1 through 4 label the four carbon atoms in the unit cell, atoms 1 and 2 in the one layer, atoms 3 and 4 in the adjacent layer in the *AB* stacking of pure graphite as shown in Fig. 5.

TABLE I. Correspondence of tight-binding overlap integrals to band parameters in the literature for graphite.

Band parameters in literature	Corresponding tight-binding overlap integrals
γ_0 (2.8−3.2 eV)	1-2[a] intralayer
γ_1 (0.27−0.40 eV)	1-3 interlayer
γ_3 (0.14−0.29 eV)	2-4 interlayer
γ_4 (0.2−0.3 eV)	1-4, 2-3 interlayer
$\gamma_2/2$ (0.019 eV)	2-2 interlayer
$\gamma_5/2$	1-1 interlayer

[a]1-2,1-3, . . . referred to the labels in Fig. 5.

In the model calculation of oxygen-intercalated graphite, a stage-1 configuration of C:O ratio equal to 2 was considered, that is, each oxygen layer is flanked by two adjacent layers of carbon atoms of the *same* stacking; the primitive cell consists of two carbon atoms and one oxygen atom. Two distinct geometrical sites of oxygen in relation to the carbon

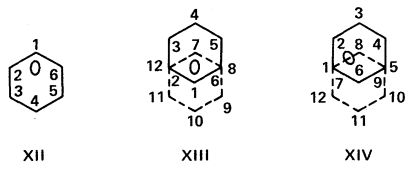

FIG. 4. Clusters modeling oxygen position site *D*. The upper graphite layer (C_7,C_8,C_9,C_{10},C_{11},C_{12}) in structures XIII and XIV is indicated by dashed lines with the oxygen atom located between the two layers.

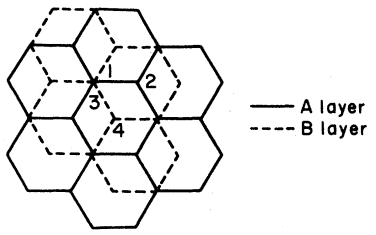

FIG. 5. Pure-graphite configuration for the tight-binding calculation.

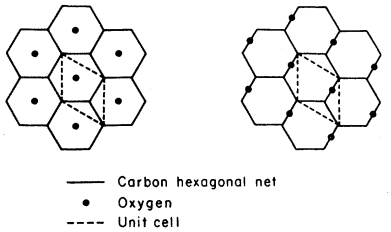

FIG. 6. Oxygen-intercalated graphite configurations. (i) Oxygen on hexagonal center site (left), and (ii) oxygen on hexagonal bridge site (right).

atoms were considered: (i) the oxygen sits at the equivalent center of the hexagonal carbon network, and (ii) the oxygen sits at the equivalent bridge site of the hexagonal network formed by carbon atoms. Both configurations (i) (left-hand graph) and (ii) (right-hand graph) are shown in Fig. 6. The Brillouin zone (BZ) is identical to that of pure graphite as shown in Fig. 7. However, the basis states of the tight-binding Hamiltonian now include the p_x, p_y, and p_z orbitals on the oxygen atom in addition to the p_z orbitals used for pure graphite. The Hamiltonian matrix elements are the overlap integrals between these basis states. Since convenient formulas for two center integrals such as $pp\sigma$, $pp\pi$, and $sp\sigma$ in terms of Slater-type atomic orbitals are available in the literature,[14] we obtained the matrix elements by evaluating two center integrals of carbon-carbon and carbon-oxygen. Analytic self-consistent-field (SCF) ground states for atomic carbon and oxygen as tabulated by Clementi *et al.*[15] were used in the calculation. The values of these integrals are then scaled with respect to the two center integrals of the pure-graphite configuration since only the band parameters that fit the Fermi surface of pure graphite are known. The carbon-oxygen interlayer distance is estimated to be 2.85 Å by assuming oxygen and carbon to be touching spheres with the radius of the carbon being an effective van der Waals radius derived from the pure-graphite geometry and the radius of the oxygen being its ionic radius.

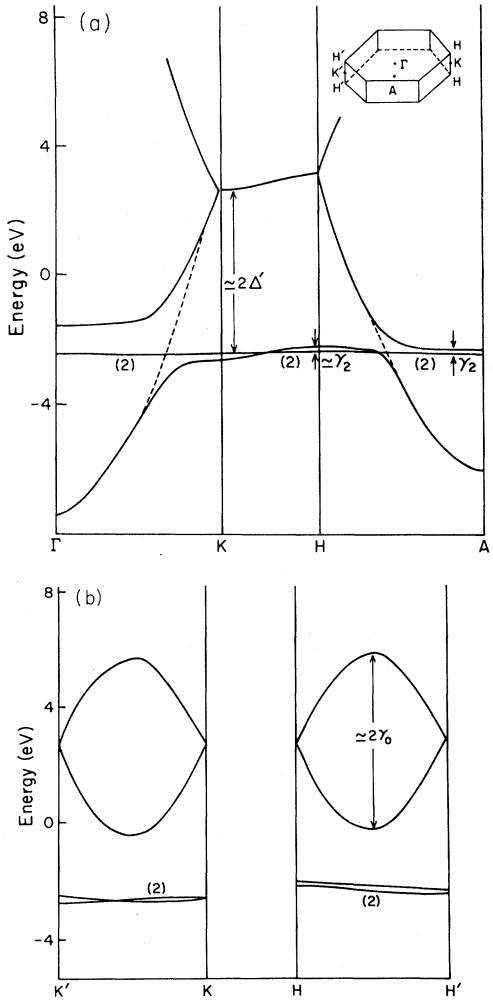

FIG. 7. (a) Band structure along Γ-*K*-*H*-*A* of oxygen-intercalated graphite for oxygen at the hexagonal center site. (b) Band structure in the direction *K*-*K*′ and *H*-*H*′ of oxygen-intercalated graphite for oxygen at the hexagonal center site.

III. RESULTS AND DISCUSSION

A. Cluster model

The various clusters chosen to model a single layer of the graphite lattice together with the calculated average binding energy per atom and the valence charge are presented in Fig. 8. For the three-dimensional graphite models with an inter-

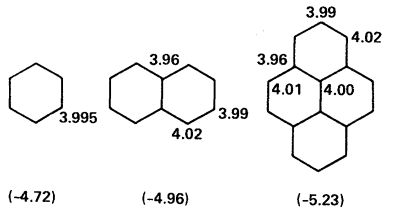

FIG. 8. Clusters modeling the graphite lattice with the calculated valence charge indicated. Binding energies are reported for each structure in units in eV/atom enclosed in parenthesis.

TABLE II. Calculated net charges at each atom for cluster models of the oxygen-graphite system, site *A*. Carbon numbering sequence refers to Fig. 1. For the three-dimensional lattice model, the oxygen-lattice distance, *d*, refers to the lower lattice plane. Oxygen binding energy, *E*, is given in eV. Because of the peripheral hydrogens, the charges below do not necessarily add up to zero.

	I	II		III	IV	
O	−0.5951	−0.5971	−0.5921	−0.6222	−0.6042	−0.5988
C_1	0.2402	0.2314	0.2189	0.2127	0.2250	0.1734
C_2	0.2273	0.1644	0.1617	0.2336	0.1358	0.0820
C_3	−0.1463	−0.1325	−0.1256	−0.1018	−0.1115	−0.0574
C_4	0.1874	0.1669	0.1620	0.0978	0.1281	0.0655
C_5	−0.1463	−0.1560	−0.1495	−0.0481	−0.1288	−0.0731
C_6	0.2273	0.2602	0.2556	0.1422	0.2111	0.1351
C_7					0.1148	0.1455
C_8					0.0566	0.1262
C_9					−0.0216	−0.0647
C_{10}					0.0296	0.0881
d (Å)	1.4139[a]	1.4139	1.4436[a]	1.4139	1.4436	1.6750
E (eV)	−0.587	−0.139	−0.155	−0.204	−0.163	−0.402

[a]Oxygen-lattice distance optimized.

layer spacing of 3.35 Å, the valence charge did not differ from the analogous two models. The good agreement between the calculated valence charges for the lattice models and the ideal graphite value, which is 4 for each carbon atom, indicates that with proper treatment of edge atoms even small clusters can adequately simulate the extended lattice.

For the oxygen-graphite models, results consisting of the net atomic charges and oxygen binding energies at indicated oxygen to lattice distances are summarized in Tables II–V. The net charge at an atom is defined as the valence charge calculated from Mulliken populations, less 4 for each carbon, and less 6 for each oxygen. Because of the peripheral hydrogens introduced for the purpose of minimizing edge effect, these net charges do not necessarily add up to zero exactly. The most stable position for the oxygen atom is predicted to be above a carbon–carbon bond at a distance of 1.25 Å for both the independent-layer and the three-dimensional lattice models. This is shown in Fig. 3 (site *C*). Charge is transferred from the nearest in-

TABLE III. Calculated net charge at each atom for cluster models of the oxygen-graphite system, site *B*. Carbon numbering sequence refers to Fig. 2. For the three-dimensional lattice model, the oxygen-lattice distance, *d*, refers to the lower lattice plane. Oxygen binding energy, *E*, is reported in eV. All oxygen-lattice distances were optimized.

	V	VI	VII
O	−0.5921	−0.6556	−0.5964
C_1	0.2189		0.2254
C_2	0.1617		0.1543
C_3	−0.1256		−0.1252
C_4	0.1620		0.1538
C_5	−0.1495		−0.1474
C_6	0.2556		0.2456
C_7		0.1706	0.0351
C_8		0.1706	0.0357
C_9		0.1706	0.0352
C_{10}		0.1706	0.0338
d (Å)	1.4436	1.0515	1.4212
E (eV)	−0.155	2.132	0.565

TABLE IV. Calculated net charges at each atom for cluster models of the oxygen-graphite system, site *C*. Carbon numbering sequence refers to Fig. 3. For the three-dimensional lattice model, the oxygen-lattice distance, *d*, refers to the lower lattice plane. Oxygen binding energy, *E* is given in eV.

	VIII	IX		X	XI	
O	−0.4453	−0.4577	−0.4618	−0.4646	−0.4600	−0.4606
C_1	0.2817	0.3063	0.3033	0.2838	0.2993	0.2989
C_2	−0.0450	−0.0638	−0.0620	−0.0161	−0.0653	−0.0651
C_3	0.0190	0.0206	0.0212	−0.0025	0.0207	0.0208
C_4	0.0190	0.0206	0.0212	−0.0025	0.014	0.0144
C_5	−0.0450	−0.0638	−0.0638	−0.0161	−0.0571	−0.0568
C_6	0.2817	0.3063	0.3033	0.2838	0.2875	0.2869
C_7				−0.0007		
C_8				−0.0038		
C_9					0.0537	0.0039
C_{10}					0.0326	0.0031
C_{11}					0.0047	0.0051
C_{12}					0.0090	0.0038
d (Å)	1.2318[a]	1.2318	1.2511[a]	1.2318	1.2511	1.2537[a]
E (eV)	−2.756	−1.774	−1.783	−1.408	−1.336	−1.336

[a]Oxygen-lattice distances optimized.

plane carbon to the oxygen atom by almost half of an electron. Comparing the results for the various models of this oxygen-graphite site in Table IV, one sees that the oxygen-lattice distances and charge distributions do not change significantly from the poorest model (VIII) where the oxygen is above an edge bond to the best model (X) where there are at least two shells of outer carbons about the bonding site. The local nature of this oxygen interaction with the nearest two carbons is thus evident. The carbon-oxygen distance and charge distributions are typical of those found in epoxide molecules.

Considering the next favored position consisting of an oxygen above a carbon atom, in the three-dimensional lattice model this position gives rise to two sites (*A*,*B*) as described below. For site *A* (Fig.

TABLE V. Calculated net charges at each atom for cluster models of the oxygen-graphite system, site *D*. Carbon numbering sequence refers to Fig. 4. For the three-dimensional lattice model, the oxygen-lattice distance, *d*, refers to the lower lattice plane. Oxygen binding energy, *E*, is reported in eV.

	XII	XIII		XIV
O	−0.5302	−0.5292	−0.5454	−0.5198
C_1	0.2001	0.1972	0.1248	0.1270
C_2	0.3143	0.2913	0.1337	0.1111
C_3	−0.2107	−0.1958	−0.0455	−0.0316
C_4	0.2257	0.1960	0.0694	0.0490
C_5	−0.2107	0.2913	−0.0455	−0.0327
C_6	0.3143	0.1972	0.1337	0.1097
C_7		0.0694	0.1248	0.1932
C_8		0.0412	0.1337	0.1375
C_9		−0.0005	−0.0455	0.0152
C_{10}		0.0128	0.0694	−0.0035
C_{11}		−0.0005	−0.0455	0.0331
C_{12}		0.0412	0.1337	−0.0309
d (Å)	1.2702[a]	1.2702	1.6750	1.6750
E (eV)	−0.336	0.030	0.362	−0.406

[a]Oxygen-lattice distance optimized.

1), where the oxygen is above and below a carbon atom, comparison of the calculations with the oxygen at the single plane optimized oxygen to lattice distance and at the point midway between the two lattice layers indicates that the charge on the oxygen (−0.60 electron) does not differ significantly from the single-plane results. However, major differences between the two- and three-dimensional lattice models are evident in the overall charge distribution summarized in Table II. With the single-layer models, the oxygen charge is at the expense of the carbon directly below the oxygen as well as those atoms adjacent to this carbon. The presence of the second carbon layer in the three-dimensional model allows for the charge on the oxygen to come from carbons on both layers leading to changes only at centers directly bonded to the oxygen and the stabilization of the larger oxygen-to-lattice distance of 1.67 Å. For the single-layer case, the smaller oxygen-lattice distance of 1.44 Å is favored. Analogous carbon-oxygen interactions found in molecules are the ether compounds with carbon-oxygen distances of 1.4−1.5 Å and carbonyls, with carbon-oxygen distances of 1.2 Å.

For the alternate site, *B* (Fig. 2), where the oxygen is located above one carbon and below the center of the hexagaonal ring of carbons, results indicate a less favored position over that of site *A*. The destabilizing effect of the oxygen unable to interact with the ring-atom charge distribution to satisfy bonding requirements is evidenced by the positive oxygen-to-lattice binding energy for the three-dimensional model (VII) and the two-dimensional model (VI).

Calculations done on models of the remaining oxygen site, *D* (Fig. 4), again result in a negative-charged oxygen at the expense of the nearest carbon atoms. For the three-dimensional model, unlike the site-*A* case, placement of the oxygen at the midpoint between the lattice layers does not result in a lowering of the energy but rather an increase indicating a preferred interaction with only a single graphite layer. This is further supported by the drastic lowering of energy when a bond site position is now made accessible to the oxygen from the upper plane as in cluster XIV.

Results of the present single-lattice calculations compare favorably with the three previous theoretical treatments of the oxygen-graphite system[9,16,17] even though different clusters were treated and the more approximate complete neglect of differential overlap (CNDO) semiempirical molecular-orbital method was used. The main difference in the three previous calculations were in the approaches used to model the extended lattice. Bennett, McCarroll, and Messmer[16] simulated the extended layer by imposing periodic boundary conditions to small clusters of carbon atoms. Dovesi *et al.*[9] used a tight-binding crystalline-orbital approach to study periodic overlayers of atomic oxygen on graphite. The work of Hayns[17] employed a cluster approach similar to ours for the two-dimensional lattice models. All three calculations were in agreement with the present results showing the bond site to be most stable followed by the atom site. Direct comparison of energies was not possible since it is well known that the CNDO approximation consistently overestimates the binding energy. Additionally, in the MINDO approximation parameters had been adjusted to give the best fit to experimental enthalpies at 298 K, and hence would somehow incorporate macroscopic dynamical effects into a static molecular calculation. The closer agreement to the experimental value of the lattice cohesive energy using the MINDO approximation compared with the CNDO approach may be due to this parametrization. The choice of parameters could also explain the discrepancy between the present results and the calculations of Hayns for a system at 0 K predicting oxygen binding at the site-*D* position. Comparison of the present calculations with the previous theoretical treatments is summarized in Tables VI and VII.

B. Band model

Since the tight-binding Hamiltonian of graphite in terms of overlap integrals has matrix elements identical in form to the Slonczewski-Weiss-McClure Hamiltonian, we have ascribed to the well established γ parameters their physical meaning in the tight-binding context in Table I. Hence γ_0 takes on the meaning of an intralayer C-C overlap integral, γ_1, γ_3, and γ_4 take on the meaning of adjacent

TABLE VI. Comparison of the oxygen atom charge for the oxygen atom above a carbon atom, a carbon−carbon bond, and the center of the hexagonal ring. All results are for single-layer models.

	Atom	Bond	Center
Present results:			
Single ring	−0.60	−0.45	−0.66
Two rings	−0.60	−0.46	
Four rings	−0.62	−0.47	
Reference 16	−0.40	−0.25	−0.19
Reference 9	−0.30	−0.25	−0.30

TABLE VII. Comparison of the oxygen-graphite equilibrium distance for the oxygen atom above a carbon atom, a carbon–carbon bond, and the center of the hexagonal ring. All results are for single-layer models.

	Atom	Bond	Center
Present results:			
Single ring	1.41	1.23	1.05
Two rings	1.44	1.25	
Reference 16	1.50	1.25	1.00
Reference 9	1.45	1.20	0.80
Reference 17		1.25	

layer-interlayer overlap integrals, and γ_2 and γ_5 take on the meaning of every other layer-interlayer overlap. In the case of oxygen-intercalated graphite, the Hamiltonian will consist of p_z-p_z overlap integrals between atoms of similar geometries as that of graphite, therefore, the same notations γ_0, γ_2, γ_5, and γ_3 are retained. A new parameter γ_6 is added to denote the p_z-p_σ (p_xp_y of 0) overlap between CO. Specifically, then, the tight-binding parameters for the oxygen-intercalated graphite are γ_0—intralayer p_z-p_z between carbon-carbon (C-C), $\gamma_2/2$—interlayer p_z-p_z between oxygen-oxygen (O-O) separated by one carbon layer, $\gamma_5/2$—interlayer p_z-p_z between C-C separated by one oxygen layer, γ_7—interlayer p_z-p_z between C-O, γ_6—interlayer p_z-p_σ between C-O, and $2\Delta'$—energy difference between the $2p$ atomic orbitals for C and O.

The parameters γ_0 and γ_5 occur also in the pure-graphite Hamiltonian so that the values in Table I can be used; values of γ_2, γ_7, and γ_6 are scaled from the SCF two-center integrals as computed for C-C, C-O, and O-O. The scaling is feasible since the overlap parameter for C-C can be determined from both the Fermi-surface measurements as shown in Table I and from the computation of SCF two-center integrals, therefore the measured and computed values for C-C are used as the reference from which we scale SCF two-center integrals of C-O and O-O to obtain γ_2, γ_7, and γ_6 to be used in our Hamiltonian. The scaled value of γ_7 for C-O is almost identical to that of γ_3 for C-C in Table I; γ_2 is one-tenth of γ_5 and γ_6 is four-tenths of γ_7. Calculations are carried out for the stage-1 intercalated graphite with the configuration as shown in the left-hand graph in Fig. 6 [hereafter referred to as (i)], where the oxygen atom is situated at the center of the carbon hexagonal net. The resultant band structure is shown in Fig. 7. Figures 7(a) and 7(b) refer to band structure in two orthogonal directions in the BZ. In order to illustrate clearly the change near the Fermi surface of pure graphite produced by the intercalation, these figures show only the bands arising from the oxygen p states and the carbon p_z states. The energies of the oxygen s states and the carbon sp^2 states are too low to be shown. There are a total of six p electrons per unit cell (two p_z electrons from the two carbons and four electrons from the oxygen) to occupy the three lowest bands in Figs. 7(a) and 7(b). The properties of these bands can be understood as follows: (a) If there were no interaction between C and O, then the oxygen p states form flat bands at about -2.0 eV. The doubly-degenerated bands denoted by (2) in Fig. 7 are the p_x and p_y bands. The carbon p_z bands are doubly degenerate along KH and are located above and separated from the oxygen p_x-p_y bands by $2\Delta'$ (the SCF atomic calculations give $2\Delta' \simeq 5.6$ eV). In the directions perpendicular to KH, one band rises rapidly while the other band falls as $\bar{k}$ toward points A and Γ due to the intralayer C-C interaction γ_0. The falling bands are indicated by the dashed lines. (b) When the C-O interaction is present, the p_z bands of oxygen hybridize with the carbon p_z bands. That is, the falling p_z band from H becomes the oxygen p_z band near A while the lowest band at A changes its character from carbon p_z state to oxygen p_z state. Similar hybridization occurs in the direction of ΓK. The interlayer C-O interaction γ_6 and γ_7 induces an insulating gap along ΓK. However, along HA, such a gap inducing interaction is nullified by the zero structure factor in the Hamiltonian matrix elements. Therefore, the energies of oxygen p_z states at H and A are degenerate. Since the six p electrons can only occupy the lowest three bands at $T=0$ K, the band structure is that of a zero-indirect-gap semiconductor. For finite T, some of the electrons can populate the band above the oxygen p_x-p_y bands near A. As we compare the curvature of the bands near A and H to the one indicated by the dashed line, the effective masses of the electrons and holes in the intercalated sample are larger than the pure graphite. Therefore, intercalation has brought in the desired result: to reduce the conductivity.

The band structure for the configuration shown in the right-hand graph of Fig. 6 [hereafter referred to as (ii)], where the oxygen is allowed to occupy the equivalent bridge site of the hexagonal carbon net, was also calculated. The configuration (ii), which was also studied by the MINDO/3 method, differs from configuration (i) in the additional interaction between the p_z orbitals of carbon with the p_x and p_y states of oxygen. This interaction induces a splitting of the oxygen doubly degenerate states along

ΓK. Otherwise, the qualitative features of the bands for configurations (i) and (ii), including the nullification of the C-O interaction along *HA* are similar. Since the splitting due to the breaking of symmetry is small on the energy scale of Fig. 7, we omit a separate figure for the band structure of configuration (ii) with the oxygen at the bridge site.

Our tight-binding calculations therefore show that, whereas the C-O interaction definitely give rise to an appreciable insulating gap along ΓK, the zero structure factor in the Hamiltonian matrix elements containing C-O interactions (γ_7 and γ_6) is responsible for the zero indirect gap along *HA*. The zero structure factor is specific to the symmetry of a stage-1 intercalation configuration where the oxygen and carbon layer separation is exactly one-half of the unit-cell length along the $\hat{c}$ direction. For higher-stage intercalation, the structure factor of the matrix elements containing the C-O interactions (γ_7 and γ_6) is no longer zero and a finite insulation gap similar to that shown in Fig. 7 for direction ΓK will be expected to occur also along *HA*. This will give rise to a finite-gap semiconductor.

In conclusion, the MINDO/3 cluster calculations suggest that the most stable position for the intercalating oxygen atoms to be 1.25 Å above a C—C bond. Therefore, it is not energetically favorable to form CO or CO_2 molecules if the carbon hexagonal net is maintained. The tight-binding band calculation predicts that the bridge-site oxygen-intercalated stage-1 graphite will be a zero-indirect-gap semiconductor. As the stage number increases, the intercalated sample can become a finite-gap semiconductor. These features are independent of the C-O separation. However, the actual value of the gap for the higher-stage intercalated sample will be governed by the C-O interactions (γ_7 and γ_6) these are functions of the separation. Therefore, our joint MINDO/3 and the tight-binding calculations show that it is possible to intercalate oxygen at the bridge site in graphite to reduce its conductivity.

ACKNOWLEDGMENTS

This work was supported by the National Aeronautics and Space Administration Ames Research Center under Contracts Nos. NAS2-10188, NAS2-10789, and NASA2-10258, and Air Force Office of Scientific Research Grant No. 77-3390.

---

*Present address: Data General Corp., Sunnyvale, CA 94086.

†To whom correspondence should be sent.

‡Present address: Building 90, Earth Sciences Division, Lawrence Berkeley Laboratory, Berkeley, CA 94720.

[1]M. S. Dresselhaus, G. Dresselhaus, J. E. Fisher, Phys. Rev. B 15, 3180 (1977), and references therein.

[2]W. Rüdorff, in *Advances in Inorganic Chemistry and Radiochemistry,* edited by H. J. Emeléus and A. G. Sharpe (Academic, New York, 1959), Vol. 1, p. 223.

[3]A. Clauss, R. Plass, H. P. Boehm, and U. Hofmann, Z. Anorg. Allg. Chem. 291, 205 (1957).

[4]R. C. Bingham, M. J. S. Dewar, and D. H. Lo, J. Amer. Chem. Soc. 97, 1285 (1975).

[5]J. C. Slater and G. F. Koster, Phys. Rev. 94, 1498 (1954).

[6]N. A. W. Holzwarth, Phys. Rev. B 21, 3665 (1980).

[7]MINDO/3 program from National Resource for Computational Chemistry, Lawrence Berkeley Laboratory, Berkeley, California.

[8]M. Kanter, Phys. Rev. 107, 655 (1955).

[9]R. Dovesi, C. Pisani, F. Ricca, and C. Roetti, Surf. Sci. 75, 316 (1978).

[10]R. S. Mulliken, J. Chem. Phys. 23, 1833 (1955).

[11]J. C. Slonczewski and P. R. Weiss, Phys. Rev. 109, 272 (1958).

[12]J. W. McClure, Phys. Rev. 108, 612 (1957).

[13]J. W. McClure, in *The Physics of Semimetals and Narrow Gap Semiconductors,* edited by D. L. Carter and R. T. Bate (Pergamon, New York, 1971), p. 127.

[14]C. C. J. Roothaan, J. Chem. Phys. 19, 1445 (1951).

[15]E. Clementi, C. C. J. Roothaan, and M. Yoshmine, Phys. Rev. 127, 1618 (1962).

[16]A. J. Bennett, B. McCarroll, and R. P. Messmer, Phys. Rev. B 3, 1397 (1971).

[17]M. R. Hayns, Theor. Chim. Acta 39, 61 (1975).